PHYSICAL REVIEW B VOLUME 62, NUMBER 22 1 DECEMBER 2000-II

Lattice dynamics and thermodynamic properties of the β-Sn phase in Si

Mathias Ekman, Kristin Persson, and Göran Grimvall
Theoretical Physics, Department of Physics, Royal Institute of Technology, SE-100 44 Stockholm, Sweden

(Received 26 April 2000)

The lattice dynamics of silicon in the metastable β-Sn structure is studied using the density-functional linear-response theory. The Grüneisen parameters and thermal expansion are calculated in the quasiharmonic approximation for the cubic diamond (cd) and β-Sn phase and the thermodynamic properties are compared with the liquid phase at zero pressure. We relate the anomalously high entropy of fusion in Si to the difference in entropy between the β-Sn and the cd phase. The melting temperature and phase boundary slopes for the β-Sn phase at zero pressure are qualitatively different from those deduced from the experimental pressure-temperature phase diagram. This suggests that the reported experimental liquid-metallic solid phase boundary does not refer to the β-Sn phase.

I. INTRODUCTION

The normal solid phase of Si has the cubic diamond (cd) lattice structure and is semiconducting, while *ab initio* electron structure calculations[1–7] have shown that the sc, fcc, bcc, sh, hcp, and β-Sn lattice structures are more or less metallic, as is also the liquid state. Those *ab initio* calculations refer to static lattices at zero Kelvin and the thermodynamic properties of the metallic solid phases have not been much studied. It is well-known that Si under pressure transforms into a variety of stuctures. With increasing pressure the sequence is: cd, β-Sn, $Imma$, sh, $Cmca$, hcp, fcc.[8] In this work we show that the sc, fcc, bcc, and sh structures are dynamically (i.e., mechanically) unstable at ambient pressure. The hcp structure has previously been shown to be unstable.[4] Hence these phases do not have a well defined Gibbs energy at zero pressure. However, the β-Sn phase of Si, which is sixfold coordinated with some covalent character to the binding,[1] is metastable until above melting. The vibrational phonon spectrum is calculated in the quasiharmonic approximation using the density-functional linear-response theory (DF-LRT). From that result, the thermal expansion coefficient and the atomic vibrational amplitude are calculated as a function of temperature, in excellent agreement with experiment for cd Si. Furthermore, the Gibbs energy is obtained, which makes possible a comparison of the metallic solid and liquid phases, when the properties of the liquid are taken from experiments. The calculated slopes of the β-Sn–cd and β-Sn–liquid phase transformation boundaries and the melting temperature of β-Sn phase at zero pressure suggest a revaluation of the experimental phase diagram.[9] In relation to the phase diagram we consider the possibility to observe the metallic phase by rapid quenching of the liquid under pressure. Finally, the anomalously high entropy of fusion observed[10,11] for Si as well as for Ge and binary semiconductors is discussed.

II. FORMALISM

In the Helmholtz free energy $F(V,T)=U(V,T)-TS(V,T)$ the most important contribution to the entropy $S(V,T)$ arises from lattice vibrations. For the metallic β-Sn phase there is also a part due to electronic excitations. We make a Sommerfeld approximation for the electronic contribution and express the free energy as

$$F(V,T)=U_0(V)-\frac{\pi^2}{6}D(\epsilon_F)k_B^2T^2+F_{\mathrm{vib}}, \tag{1}$$

where U_0 is the energy at $T=0$, uncorrected for zero-point vibrations, $D(\epsilon_F)$ is the electron density of states at the Fermi level and the vibrational part is obtained[12] as

$$F_{\mathrm{vib}}=k_BT\sum_{\mathbf{q},s}\ln\left\{2\sinh\left[\frac{h\nu_s(\mathbf{q},V)}{2k_BT}\right]\right\}. \tag{2}$$

In order to get the equation of state from Eq. (1) we calculate the volume dependence of the mode phonon frequencies, $\nu_s(\mathbf{q},V)$, using state-of-the-art DF-LRT. The mode Grüneisen parameters $\gamma_s(\mathbf{q})=-\partial\ln\nu_s(\mathbf{q},V)/\partial\ln V$ are extracted by taking the finite differences between the phonon frequencies calculated at two volumes separated by 2%. The equilibrium volume V_{eq} as a function of temperature can now be obtained from the equation of state at zero pressure. Since the change in the c/a ratio for the β-Sn structure is almost negligible for volumes reached by thermal expansion, we use the expression

$$\alpha(T)=\frac{1}{3V_{\mathrm{eq}}}\left(\frac{\partial V_{\mathrm{eq}}}{\partial T}\right), \tag{3}$$

to estimate the linear thermal expansion coefficient in all directions for both the cd and the β-Sn phases. The thermal average of the displacement $\langle u_j^2(\kappa)\rangle$ in the j direction, can be calculated from the mode frequencies $\nu_s(\mathbf{q})$ and their polarizations $\epsilon_{j,s}(\mathbf{q},\kappa)$ as[13]

$$\langle u_j^2(\kappa)\rangle=\frac{1}{4\pi^2N_cM_\kappa}\sum_{\mathbf{q},s}\frac{E_s(\mathbf{q})}{\nu_s^2(\mathbf{q})}\epsilon_{j,s}(\mathbf{q},\kappa)\epsilon_{j,s}^*(\mathbf{q},\kappa), \tag{4}$$

where $E_s(\mathbf{q})=\frac{1}{2}h\nu_s(\mathbf{q})\coth[h\nu_s(\mathbf{q})/2k_BT]$, N_c is the number of primitive cells in the lattice, and M_κ is the mass of atom κ. Making a high-temperature expansion for the displacement vector $\langle\mathbf{u}^2\rangle$ in a cubic crystal yields

$$\langle \mathbf{u}^2 \rangle = \frac{3k_{\mathrm{B}}T}{4\pi^2 M \nu^2(-2)}. \quad (5)$$

The moment frequency $\nu(n)$ is defined by $\nu^n(n) = (1/6N_c)\Sigma \nu^n$ for $n \neq 0$ and $\ln \nu(0) = (1/6N_c)\Sigma \ln \nu$.

III. METHOD

All results were obtained within the local-density approximation of the density-functional theory. The calculations were performed using a plane-wave basis set and separable norm-conserving pseudopotentials.[14] We used the optimization procedure of Rappe *et al.*[15] and included multiple projectors for *s*- and *p*-angular momenta as suggested by Vanderbilt[16] and Blöchl.[17] The core radii were chosen to be 2.0 a.u. and the *d* pseudopotential was chosen as the local pseudopotential. This scheme allowed a plane-wave energy cutoff $E_{\mathrm{cut}} = 25$ Ry. The total energy convergence was better than 0.1 mRy/atom. We used the conjugate gradient method to iteratively solve the Schrödinger equation[18,19] and the modified Broyden mixing scheme[20] to achieve screening self-consistency. The Brillouin-zone summations were carried out using the deVita and Gillan finite-temperature method[21] where the electronic occupation numbers are calculated from the Fermi-Dirac distribution with $T = 640$ K. We chose a $16 \times 16 \times 16$ Monkhorst-Pack[22] grid yielding 145 **k** points and 349 **k** points in the irreducible wedge of the Brillouin zone for the cd and the β-Sn structures, respectively. The c/a-ratio in the β-Sn structure was optimized for each volume.

The phonon frequencies were calculated using the DF-LRT (Ref. 23) for metallic systems.[24,25] Calculations were performed on a $16 \times 16 \times 16$ **q**-point mesh in the symmetry directions and on a complete $8 \times 8 \times 8$ **q**-point mesh in the full Brillouin zone. A cubic spline was used to interpolate between the calculated phonon frequencies to obtain the dispersion curves.

IV. RESULTS

As a first step, static properties such as lattice constants, structure energy differences, and bulk moduli, were calculated for Si in the bcc, fcc, hcp, sh, β-Sn, and cd structures. The agreement with earlier theoretical studies[2,3] was excellent. Turning to the dynamics of the crystal structures, calculations of the dispersion relations in the high-symmetry directions show that all the metallic structures in this study, except the β-Sn phase, exhibit unstable modes at zero pressure. Table I summarizes the unstable modes in the high-symmetry directions, and the corresponding transformation paths. In the sc and sh structure the elastic constant $C' = \frac{1}{2}(C_{11} - C_{12})$ is positive but it couples to the TA(X) and $\mathrm{TA}_{[010]}(L)$ phonon modes, respectively, and becomes negative when the crystal is distorted according to these phonons. The sc→sh and the sh→β-Sn phase transformations require careful optimization of the elastic constant together with the phonon mode. Note that all the studied phases are unstable towards the sh lattice, which in turn is unstable towards the β-Sn lattice. The pressure-stabilized β-Sn phase has not been seen in experiments at zero pressure as it transforms upon unloading to a number of fourfold and fivefold-coordinated metastable semimetallic and semiconducting phases.[27] In Fig. 1 we present the calculated mode Grüneisen parameters $\gamma_s(\nu)$ in the complete Brillouin zone together with the phonon density of states at the equilibrium volume for the cd and the β-Sn structures of Si. Compared to the ground-state structure of Si (cd), the mode Grüneisen parameters in the β-Sn phase exhibit higher positive and fewer negative values. Since there are no unstable phonon modes we conclude that the β-Sn phase, although it has not been seen at ambient conditions, is a dynamically stable (i.e., thermodynamically metastable) phase in Si. According to earlier studies[2,28,29] on metastable phases of Si, the β-Sn phase has the most metallic character among these structures.

TABLE I. Instabilities in the metallic phases of Si at their respective equilibrium volume. All symmetry points and phonon vectors are given on the same Bravais lattices as in Ref. 26.

Structure	Unstable mode	Path	
bcc	C'		
	LA $(\frac{2}{3}[111])$	LA $(\frac{2}{3}[111])$	$\rightarrow \omega$
	TA_1 (N)	TA_1 $(N) + C'$	→hcp
	TA_2 (N)	TA_2 $(N) + C'$	→sh
fcc	C'		
	TA (X)	TA $(X) + C'$	→sh
sc	TA (X)	TA $(X) + C'$	→sh
hcp	TO (A)	TO (A)	→sh
sh	$\mathrm{TA}_{[010]}$ (L)	$\mathrm{TA}_{[010]}$ $(L) + C'$	→β-Sn

[a] Reference 4.

To identify some of the anomalous modes in the β-Sn phase, we show in Fig. 2 the calculated mode Grüneisen parameters $\gamma_s(\mathbf{q})$ together with the phonon dispersion curves in the symmetry directions for the β-Sn phase of Si. The negative $\gamma_s(\mathbf{q})$ in β-Sn Si can be related to the instability of the structure under pressure. The LO phonon mode at the zone center transforms,[4] together with a c/a adjustment

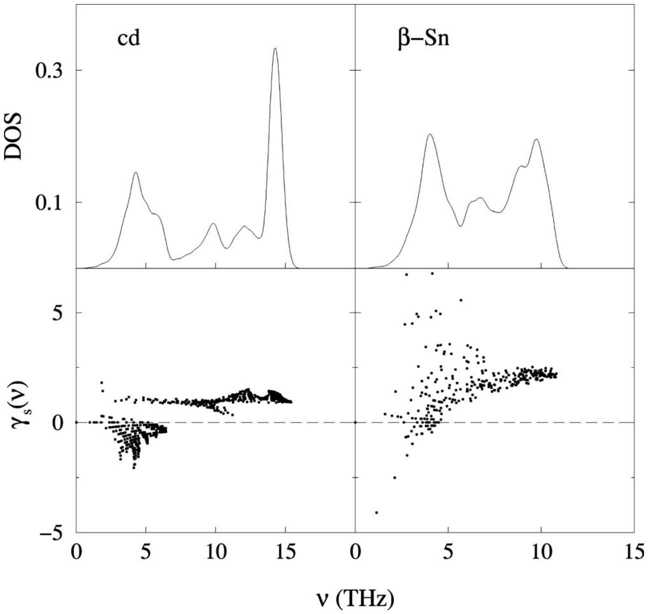

FIG. 1. Calculated phonon density of states and Grüneisen parameters of cd and β-Sn Si.

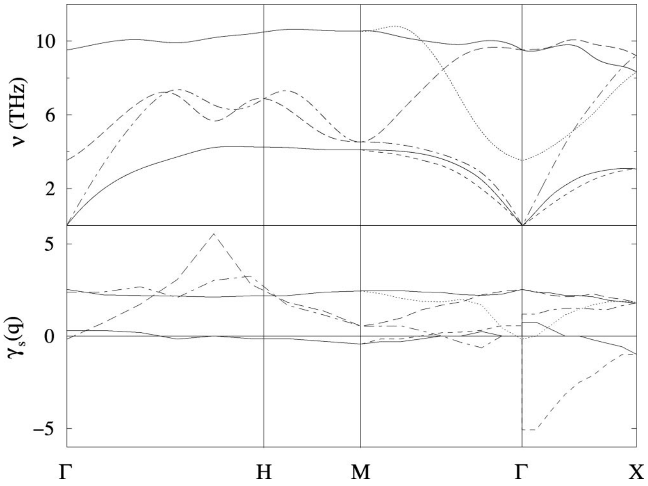

FIG. 2. Calculated phonon frequencies in the symmetry directions and the corresponding mode Grüneisen parameters of β-Sn Si. In the long-wavelength limit, we assume $\nu = C_s|\mathbf{q}|$ for the acoustic branches which gives the mode Grüneisen parameters for the Γ point as $\gamma_s(\Gamma) = -(V/C_s)(\partial C_s/\partial V) + \frac{1}{3}$. Hence the value of $\gamma_s(\Gamma)$ depends on the specific **q** direction from which it is calculated.

$[0.548(\beta\text{-Sn}) \rightarrow 0.535(\text{sh})]$, the β-Sn structure to the sh structure. In fact, the negative Grüneisen parameters in the $[\xi\xi 0]$ direction correspond to the pressure-induced softening of the elastic constant combination $C_{11} - C_{12}$, which is equivalent to a c/a shift. The LO$[00\frac{1}{2}]$ mode has a very high Grüneisen parameter and has recently been identified[30] as an incipient instability intrinsic to the β-Sn lattice. If unstable, it transforms the β-Sn lattice to an eight-atom tetragonal superstructure. The most positive mode Grüneisen parameters belong to a zone-boundary phonon mode, $\mathbf{q} = \text{TA}[0\frac{1}{2}\frac{1}{2}]$, outside the plotted high-symmetry directions.

The calculated thermal expansion for the cd and β-Sn structures are presented together with available experimental results for the cd phase in Fig. 3. The result for the cd phase agrees very well with experiments, indicating that the used scheme is accurate. Similar results have been obtained earlier[31] for the cd structure with the same method. We note that the thermal expansion is about four times larger in the β-Sn structure compared to the cd structure.

The cd structure has cubic symmetry and therefore an isotropic displacement $\langle u_j^2 \rangle$, shown as a function of temperature in Fig. 4. The β-Sn structure has axial symmetry and two independent quantities $\langle u_j^2 \rangle$, referring to vibrations along the x and z axes, respectively; see Fig. 4. In Table II we give moment frequencies $\nu(n)$ and the corresponding moment Grüneisen parameters $\gamma(n) = -\partial \ln \nu(n)/\partial \ln V$. For strictly harmonic lattice vibrations, the high-temperature displacement vector $\langle \mathbf{u}^2 \rangle$ [cf. Eq. (5)] varies linearly in T. Anharmonic effects, including the quasiharmonic shift in phonon frequencies associated with the thermal expansion, will give $\langle \mathbf{u}^2 \rangle$ a nonlinear T dependence. Figure 4 may suggest an almost harmonic behavior in the cd structure. However, the quasiharmonic shift in the frequency $\nu(-2)$ is $3\nu(-2)\gamma(-2)\alpha\Delta T$. Both the thermal expansion coefficient α and the Grüneisen parameter $\gamma(-2)$ are much smaller in the cd structure than in the β-Sn structure. The low value of $\gamma(-2)$ in cd structure is caused by a cancellation of positive and negative values of mode Grüneisen parameters when the average $\gamma(-2)$ is formed, and is not a sign of small anharmonicity; cf. Fig. 1. The high-temperature vibrational entropy depends on the moment frequency $\nu(0)$, and since $\gamma(0)$ is fairly large (Table II) the quasiharmonic correction

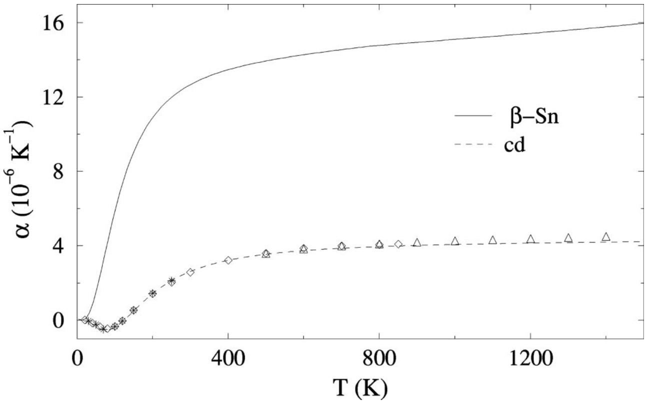

FIG. 3. Calculated and experimental thermal expansion in β-Sn and cd Si. △: Ref. 32; ◇ : Ref. 33; *: Ref. 34.

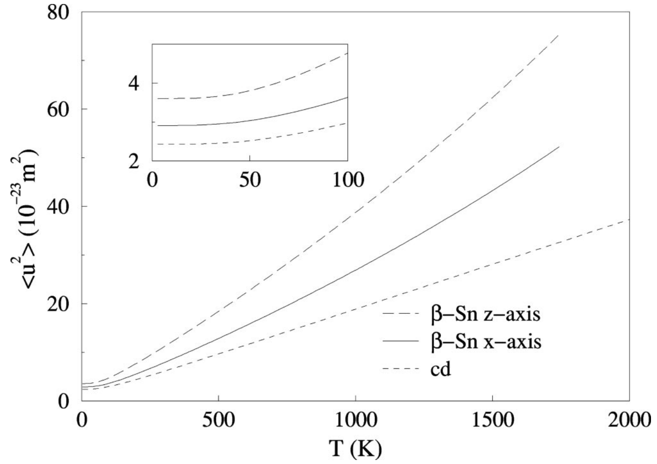

FIG. 4. Calculated vibrational amplitude in β-Sn and cd Si. The inset shows an enlargement of the same quantity for low temperatures.

TABLE II. Calculated moment frequencies $\nu(n)$ and their Grüneisen parameters $\gamma(n)$ at the equilibrium volumes, corrected for zero-point vibrations, 132.46 a.u.^{3}/atom and 101.21 a.u.^{3}/atom for the cd and β-Sn structures, respectively.

	$\nu(n)$ (THz)		$\gamma(n)$	
n	cd	β-Sn	cd	β-Sn
−2	6.24	5.21	−0.19	1.27
−1	7.41	5.74	0.13	1.54
0	8.65	6.08	0.56	1.73
1	9.84	6.75	0.88	1.88
2	10.73	7.18	1.06	1.98
3	11.37	7.53	1.13	2.04
4	11.83	7.81	1.17	2.08
5	12.17	8.04	1.18	2.10
6	12.42	8.23	1.19	2.12

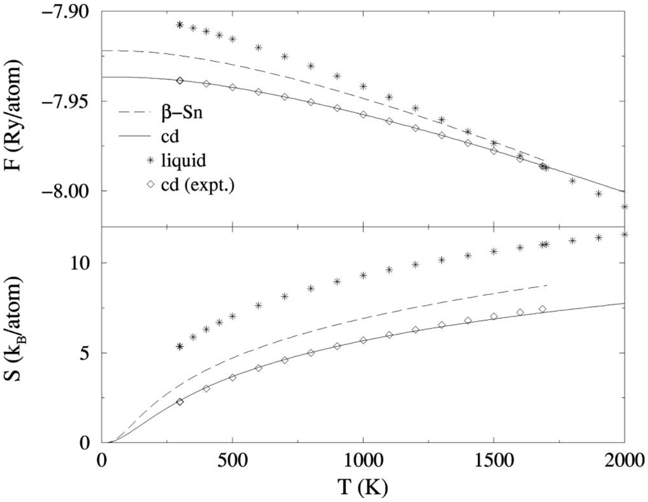

FIG. 5. Calculated (dashed and solid lines) and experimental (symbols) Helmholtz free energy *F* and entropy *S* in β-Sn and cd Si as a function of temperature. ◇ : cd, solid phase (Ref. 36); *: liquid phase (Ref. 36).

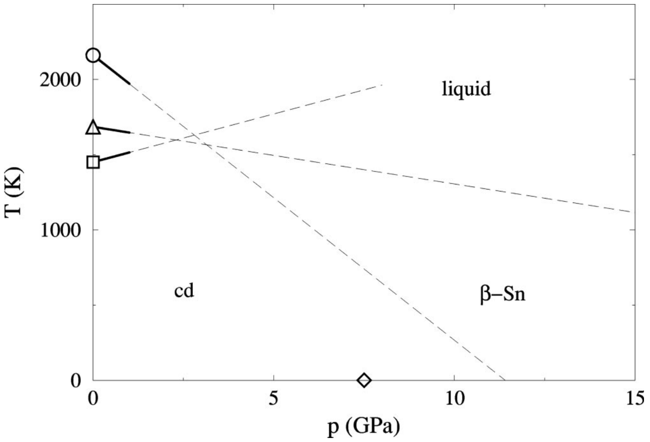

FIG. 6. Calculated end points and slopes in a schematic phase diagram for the β-Sn, cd, and liquid phases in Si. ○: extrapolated cd–β-Sn transformation temperature; △: cd melting temperature; □: β-Sn melting temperature; ◇ : cd–β-Sn calculated transformation pressure.

to the entropy can not be neglected in Fig. 5. The Debye-Waller factor derived from neutron scattering[35] on Si in the range 300–1100 K shows almost no temperature dependence in the equivalent Debye temperature, which is consistent with the very small nonlinear effects in $\langle \mathbf{u}^2 \rangle$ found here for the cd structure.

The Helmholtz free energy $F(T)$ and the entropy $S(T)$ for the β-Sn, the cd and the liquid phase (taken from experiments) at $V_{\mathrm{eq}}(T)$ are presented in Fig. 5. We note that the β-Sn phase melts at 1450 K and that the calculated thermodynamic properties for the cd phase are remarkably close to experimental values. The calculated entropy of the cd phase at the melting point is $0.2k_{\mathrm{B}}$ less than the experimental value, which we attribute to anharmonicity beyond the quasiharmonic approximation. Using the information in Fig. 5 we construct an approximate three-phase pT diagram. From ΔS and ΔV at the phase transformation temperatures the Clausius-Clapeyron relation gives the slope of the phase boundaries (solid lines which are extrapolated as dashed lines in Fig. 6) between the cd and the β-Sn phase, the cd and the liquid phase, and the β-Sn and the liquid phase, at zero pressure. Comparing the schematic phase diagram in Fig. 6 with the experimental[9] results for Si and Ge in Fig. 7 we observe the following.

(i) The calculated phase transformation boundary between the cd and the metallic β-Sn structures exhibits a negative dT/dp which agrees with the phase diagram of Ge but not with that reported for Si; cf. Fig. 7.

(ii) The calculated melting temperature of the Si β-Sn phase increases with pressure, in agreement with experiments, but the experimental value extrapolated to zero pressure is around 1000 K, which is far from the calculated 1450 K.

(iii) The estimated triple point in our calculated three-phase pT diagram (Fig. 6) for Si is located at much lower pressures and higher temperatures (3 GPa, 1600 K) than in the reported experimental Si phase diagram (15 GPa, 1100 K).

Judging from the first observation, we find it unlikely that the Si cd–β-Sn phase boundary (which in Ge, InAs, and InP exhibits[37] a negative dT/dp) should have a positive slope. The phonon frequencies in the metastable metallic β-Sn structure are much lower than in the cd structure, which will at some temperature destabilize the cd phase with respect to a hypothetic β-Sn phase at zero pressure. This is incompatible with a positive dT/dp for the Si cd–β-Sn phase boundary. Turning to the calculated liquid–β-Sn phase boundary, we observe that the high value (1450 K) of the melting temperature at zero pressure and a positive dT/dp imply that the experimental liquid-metallic phase boundary (which, if extrapolated to zero pressure yields a melting temperature of about 1000 K) cannot refer to the β-Sn phase. In order for a metallic phase (with approximately the same phonon frequencies as in Si β-Sn) to have a melting temperature of 1000 K at zero pressure, its static equilibrium energy should be about 8 mRy/atom above that of the β-Sn structure. One candidate for this is the $Cmca$ structure,[39] for which $\Delta E_{\beta\text{-Sn-}Cmca} = 9$ mRy, according to our calculations. In order to be consistent with experiments, i.e., the liquid-solid phase boundary having a negative dT/dp, (c.f. Fig. 7), the slope of the liquid–β-Sn phase boundary needs to change sign with

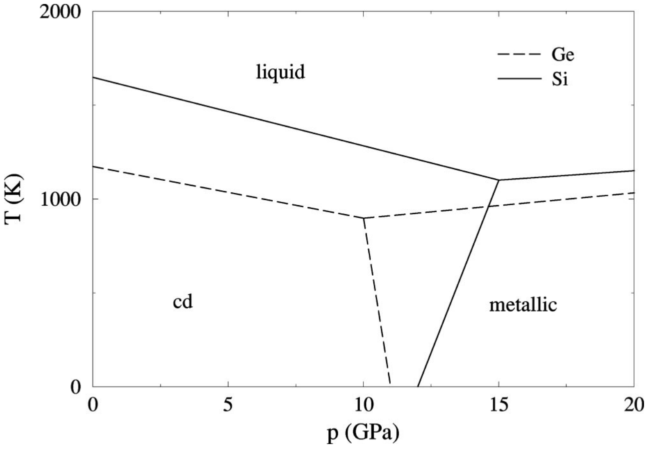

FIG. 7. Experimental (Ref. 9) pT-phase diagram for Si and Ge.

increasing pressure. According to the Clausius-Clapeyron relation, this occurs when the volumes of the two phases are equal. Assuming constant compressibility, $dT/dp=0$ at $p\sim 13$ GPa. However, there is evidence for pressure-induced liquid-liquid transitions in C,[38] which increase the density and the coordination number. If such liquid-liquid transitions occurred in Si, the liquid–β-Sn phase boundary would change drastically. Still, our calculated thermodynamic properties of β-Sn Si suggest that the first phase to appear when cooling the melt under pressure (around 8–10 GPa) should be a metallic phase like β-Sn, and not the cd structure as implied by the reported experimental phase diagram. This is likely since the electronic similarity between the β-Sn phase and the liquid state will decrease the activation barrier in the solidification process. Furthermore, the β-Sn structure has been observed as the first solid phase in undercooled Ge at 5 GPa.[40] In conclusion, our results point to the necessity of a new experimental investigation of the pT phase diagram of Si.

Following the work of Wallace,[10] the entropy of fusion is expressed as

$$\Delta S_f \approx 0.8k_{\mathrm{B}}+D, \tag{6}$$

where $0.8k_{\mathrm{B}}$ is due to the normal loss of long-range order in melting and D is attributed to the change in electronic groundstate between the solid and the liquid state. The experimental[41,42] value for $\Delta S_f/k_{\mathrm{B}}$ is $3.3-3.6$ and it has been calculated[43] to be 3.1 within the DFT-LDA formalism using *ab initio* molecular dynamics. We model the change in the electronic ground state of Si on melting by comparing the ground-state semiconducting phase with the β-Sn phase which is, to our knowledge, the most metallic dynamically stable phase of Si at ambient conditions. Wallace performs the analysis of ΔS_f at a fixed density, i.e., that of the liquid. However, it is important to make sure that all phases are still dynamically stable at this density. In the case of Si we find that a β-Sn zone-boundary phonon mode ($\mathbf{q}=\mathrm{TA}[0\,\frac{1}{2}\,\frac{1}{2}]$) softens as the volume expands. Additional linear-response calculations show that it becomes unstable at the volume 107 a.u.^{3}/atom (corresponding to V_{eq} for β-Sn at 1700 K), which is much smaller than that of the liquid, 123 a.u.^{3}/atom. Note that the entropy and the Helmholtz free energy curves in Fig. 5 for the β-Sn phase are terminated at the temperature where the lattice becomes unstable. This instability forces us to retain the large volume differences between the competing phases in our analysis of ΔS_f. At the melting temperature for the β-Sn structure we find $S(\beta\text{-Sn})-S(\mathrm{cd})=1.4\ k_{\mathrm{B}}$. Adding 0.8 k_{B} from the loss of long-range order we get 2.2 k_{B} which is still far from the observed experimental and previously calculated values. This discrepancy can be attributed to a combination of effects. The liquid is metallic, which decreases the strength of the interatomic forces and hence increases the vibrational-like entropy. However, some covalent character remains in the liquid state. That leads to a low atomic coordination number when compared with truly metallic states, and therefore to an entropy increase associated with the less dense atomic packing. Unfortunately, there is no strict separation of these two entropy contributions in the liquid.

V. CONCLUSION

We have shown that, among several simple structures in Si, the β-Sn structure is the only dynamically stable metallic state at zero pressure. The Helmholtz free energy of β-Sn and cd Si was calculated in the quasiharmonic approximation and compared with that of the liquid. In the same approximation various other thermodynamic quantities (Grüneisen parameters, phonon density of states, thermal expansion, and vibrational displacement) were calculated for the β-Sn and cd phases, in excellent agreement with available experimental data for cd Si. The resulting slopes of the β-Sn phase boundaries and the β-Sn melting temperature at zero pressure require a revaluation of the experimental phase diagram. We also propose that the experimentally observed liquid-metallic phase boundary should be attributed to a phase other than β-Sn, possibly the $Cmca$ structure. We hope that this will encourage further experimental and theoretical studies of the Si phase diagram, especially in search of pressure-induced liquid-liquid transitions and a possible liquid–β-Sn transition under pressure. The anomalously high entropy of fusion in Si has previously been attributed to the change of electronic ground state. We have modeled the liquid with the β-Sn phase and calculated the difference in entropy between the semiconducting (cd) and the metallic (β-Sn) phase at the melting temperature for Si. The result is about 1 k_{B} smaller than the experimental value. We conclude that the deviation is due to the combined effect of the much lesser density and slightly more metallic character of the liquid, which both lead to an increased entropy in the liquid compared to the β-Sn structure.

ACKNOWLEDGMENTS

This work was supported by the Swedish research foundation SSF. The calculations were performed at the Swedish primary national resource for high-performance computing and networking, Parallelldatorcentrum-PDC.

---

[1] S.P. Lewis and M.L. Cohen, Phys. Rev. B **48**, 3646 (1993).

[2] M.T. Yin and M.L. Cohen, Phys. Rev. B **26**, 5668 (1982).

[3] R.J. Needs and A. Mujica, Phys. Rev. B **51**, 9652 (1995).

[4] K.J. Chang and M.L. Cohen, Phys. Rev. B **31**, 7819 (1985).

[5] A.Y. Liu, K.J. Chang, and M.L. Cohen, Phys. Rev. B **37**, 6344 (1988).

[6] I. Štich, R. Car, and M. Parrinello, Phys. Rev. B **44**, 4262 (1991).

[7] W. Jank and J. Hafner, Phys. Rev. B **41**, 1497 (1990).

[8] For a recent review, see R. J. Nelmes and M. I. McMahon, in *High Pressure Semiconductor Physics I*, edited by T. Suski and W. Paul (Academic, New York, 1998), p. 145.

[9] F.P. Bundy, J. Chem. Phys. **41**, 3809 (1964).

[10] D.C. Wallace, Proc. R. Soc. London, Ser. A **433**, 631 (1991).

[11] A.R. Regel and V.M. Glazov, Semiconductors **29**, 405 (1995).

[12] N.W. Ashcroft and N.D. Mermin, *Solid State Physics* (W.B. Saunders Company, Philadelphia, 1976).

[13] G. Grimvall, *Thermophysical Properties of Materials* (North-Holland, Amsterdam, 1999).
[14] B. Sadigh and V. Ozoliņš (unpublished); B. Sadigh, Ph.D. thesis, Royal Institute of Technology, Sweden, 1997.
[15] A.M. Rappe, K.M. Rabe, E. Kaxiras, and J.D. Joannopolous, Phys. Rev. B **41**, 1227 (1990).
[16] D. Vanderbilt, Phys. Rev. B **41**, 7892 (1990).
[17] P. Blöchl, Phys. Rev. B **41**, 5414 (1990).
[18] M.P. Teter, M.C. Payne, and D.C. Allen, Phys. Rev. B **40**, 12 255 (1989).
[19] D.M. Bylander, L. Kleinman, and S. Lee, Phys. Rev. B **42**, 1394 (1990).
[20] G.P. Srivastava, J. Phys. A **17**, L317 (1984).
[21] M.J. Gillan, J. Phys.: Condens. Matter **1**, 689 (1990).
[22] H.J. Monkhorst and J.D. Pack, Phys. Rev. B **13**, 5188 (1976).
[23] S. Baroni, P. Giannozzi, and A. Testa, Phys. Rev. Lett. **58**, 1861 (1987); P. Giannozzi, S. de Gironcoli, P. Pavone, and S. Baroni, Phys. Rev. B **43**, 7231 (1991).
[24] V. Ozoliņš, Ph.D. thesis, Royal Institute of Technology, Sweden, 1996.
[25] S. de Gironcoli, Phys. Rev. B **51**, 6773 (1995).
[26] P. H. Dederichs, H. Schober, and D. J. Sellmyer, in *Metals: Phonon States and Electron States and Fermi Surfaces*, edited by K.-H. Hellwege and J.L. Olsen, Landolt-Börnstein, New Series, Group III, Vol. 13, Part A (Springer-Verlag, Berlin, 1981).
[27] V.E. Dmitrienko, M. Kléman, and F. Mauri, Phys. Rev. B **60**, 9383 (1999).
[28] J. Crain, S.J. Clark, G.J. Ackland, M.C. Payne, V. Milman, P.D. Hatton, and B.J. Reid, Phys. Rev. B **49**, 5329 (1994).
[29] E. Kaxiras and L.L. Boyer, Phys. Rev. B **50**, 1535 (1994).
[30] V. Ozoliņš and A. Zunger, Phys. Rev. Lett. **82**, 767 (1999).
[31] A. Fleszar and X. Gonze, Phys. Rev. Lett. **64**, 2961 (1990).
[32] Y. Okada and Y. Tokamaru, J. Appl. Phys. **56**, 314 (1984).
[33] H. Ibach, Phys. Status Solidi **31**, 625 (1969).
[34] R.H. Carr, R.D. Cammon, and G.K. White, Philos. Mag. **12**, 779 (1965).
[35] B.W. Batterman and D.R. Chipman, Phys. Rev. **127**, 690 (1962).
[36] M. W. Chase, Jr., C. A. Davies, J. R. Downey, Jr., D. J. Frurip, R. A. McDonald, and A. N. Syverud, in *JANAF Thermochemical Tables*, 3rd ed., Part II, p. 1796, Suppl. No. 1 to J. Phys. Chem. Ref. Data, Vol. 14 (National Bureau of Standards, Washington DC, 1985).
[37] A. Jayaraman, W. Klement, Jr., and G.C. Kennedy, Phys. Rev. **130**, 540 (1963).
[38] M.P. Grumbach and R.M. Martin, Solid State Commun. **100**, 61 (1996).
[39] M. Hanfland, U. Schwarz, K. Syassen, and K. Takemura, Phys. Rev. Lett. **82**, 1197 (1999).
[40] F.X. Zhang and W.K. Wang, Phys. Rev. B **52**, 3113 (1995).
[41] A.R. Ubbelohde, *The Molten State of Matter* (Wiley, New York, 1978), p. 239.
[42] I. Barin, *Thermochemical Data of Pure Substances* (VCH Verlags-AG, Weinheim, 1989), p. 134.
[43] O. Sugino and R. Car, Phys. Rev. Lett. **74**, 1823 (1995).